nature geoscience

LETTERS

PUBLISHED ONLINE: 12 MAY 2013 | DOI: 10.1038/NGEO1818

Slip weakening as a mechanism for slow earthquakes

Matt J. Ikari[1,2]*, Chris Marone[2], Demian M. Saffer[2] and Achim J. Kopf[1]

Slow slip forms part of the spectrum of fault behaviour between stable creep and destructive earthquakes[1,2]. Slow slip occurs near the boundaries of large earthquake rupture zones[3,4] and may sometimes trigger fast earthquakes[2]. It is thought to occur in faults comprised of rocks that strengthen under fast slip rates, preventing rupture as a normal earthquake, or on faults that have elevated pore-fluid pressures[5–7]. However, the processes that control slow rupture and the relationship between slow and normal earthquakes are enigmatic. Here we use laboratory experiments to simulate faulting in natural rock samples taken from shallow parts of the Nankai subduction zone, Japan, where very low-frequency earthquakes—a form of slow slip—have been observed[8–10]. We find that the fault rocks exhibit decreasing strength over millimetre-scale slip distances rather than weakening due to increasing velocity. However, the sizes of the slip nucleation patches in our laboratory simulations are similar to those expected for the very low-frequency earthquakes observed in Nankai. We therefore suggest that this type of fault-weakening behaviour may generate slow earthquakes. Owing to the similarity between the expected behaviour of slow earthquakes based on our data, and that of normal earthquakes during nucleation, we suggest that some types of slow slip may represent prematurely arrested earthquakes.

Most slow fault slip has been observed near the downdip limit of the seismogenic zone at depths of ~25–45 km (refs 2,11), but in well-instrumented areas it has also been detected at shallow depths (<10 km), updip of large earthquake ruptures[8–10]. Slow slip events at tectonic boundaries probably occur at the plate interface[2,10], and therefore should be controlled by the frictional properties and conditions that characterize fault zones. For deep slow slip events, laboratory testing of natural material under *in situ* conditions is not feasible at present. Therefore, there is very little evidence to constrain the boundary conditions and friction laws that govern how these events nucleate, propagate and ultimately arrest[12]. Less attention has been paid to slow and transient slip at shallow depths; however, these regions are accessible to drilling and sampling. Here, we focus on the Nankai Trough, Japan, where mudstone samples have been recovered from major shallow fault zones[13,14].

Very low-frequency (VLF) earthquakes observed at Nankai have reverse-faulting focal mechanisms, and occur on splay faults within the accretionary prism or along the shallow décollement[8–10]. They seem to occur in regions of elevated pore-fluid pressure and therefore decreased effective stress[11,15]. The event locations correlate approximately with the estimated updip extent of rupture from the 1944 and 1946 $M_w > 8$ great earthquakes, and with the location of scientific drillsites (Fig. 1). Shallow portions of a major splay fault (Site C0004; ~300 m depth) and the décollement (Site 1174; ~800 m depth) were penetrated during Integrated Ocean Drilling Program Expedition 316 and Ocean Drilling Program Leg 190, respectively[13,14] (Fig. 1). Brecciated hemipelagic silty claystone samples from within zones of active shearing contain 37–65% clay minerals, up to 40% quartz+plagioclase and little calcite[13,14].

Fault slip instability and earthquake nucleation are typically evaluated by combining elastic dislocation theory with friction laws[16–19]. The criterion for slip instability is derived from a force balance, in which the elastic stiffness of the loading system K (stress/length) must be smaller than a critical stiffness K_c defined by the properties of the fault. Within the framework of rate- and state-dependent (RSF) friction, the instability criterion can be written to first order as:

$$K < K_c = \frac{-(a-b)\sigma_n'}{D_c} \quad (1)$$

where σ_n' is the effective normal stress and D_c is a critical slip distance over which fault strength evolves[18]. The parameter $a-b$ is defined by the experimentally measured change in steady-state friction in response to a change in sliding velocity from V_o to V (Fig. 2):

$$a-b = \frac{\Delta\mu_{ss}}{\ln(V/V_o)}$$

Positive values of $a-b$ define velocity-strengthening behaviour, which indicates that stable sliding should be expected. Negative values of $a-b$ (velocity weakening) are a requirement for the nucleation of slip instability[17,18].

In general, the mechanism(s) that allow slow slip that is sustained and quasi-dynamic is poorly understood[12,19]. Many forms of slow slip are considered to be aseismic (for example, creep events, earthquake afterslip) and therefore are expected only on velocity-strengthening faults, and typically in response to a perturbation[20]. These non- or quasi-dynamic events would be undetected by seismometers and instead must be identified geodetically[21–23]. Others, such as VLF events, are detected seismically (that is, they radiate seismic energy), indicating a dynamic stress drop[8,9]. Laboratory work shows consistent velocity strengthening for samples from the shallow Nankai megasplay and décollement[24], which is seemingly incompatible with the occurrence of shallow VLF events, although an observed minima in $a-b$ in the velocity range ~0.3-3 $\mu m\,s^{-1}$ has been predicted to favour slow slip[24].

One aspect of friction that is typically overlooked is the effect of long-term slip hardening or weakening. In the standard RSF formulation, the slip over which friction evolves following a

[1]MARUM, Center for Marine Environmental Sciences, University of Bremen, 28359 Bremen, Germany, [2]Department of Geosciences, Pennsylvania State University, University Park, Pennsylvania 16802, USA. *e-mail: mikari@marum.de.

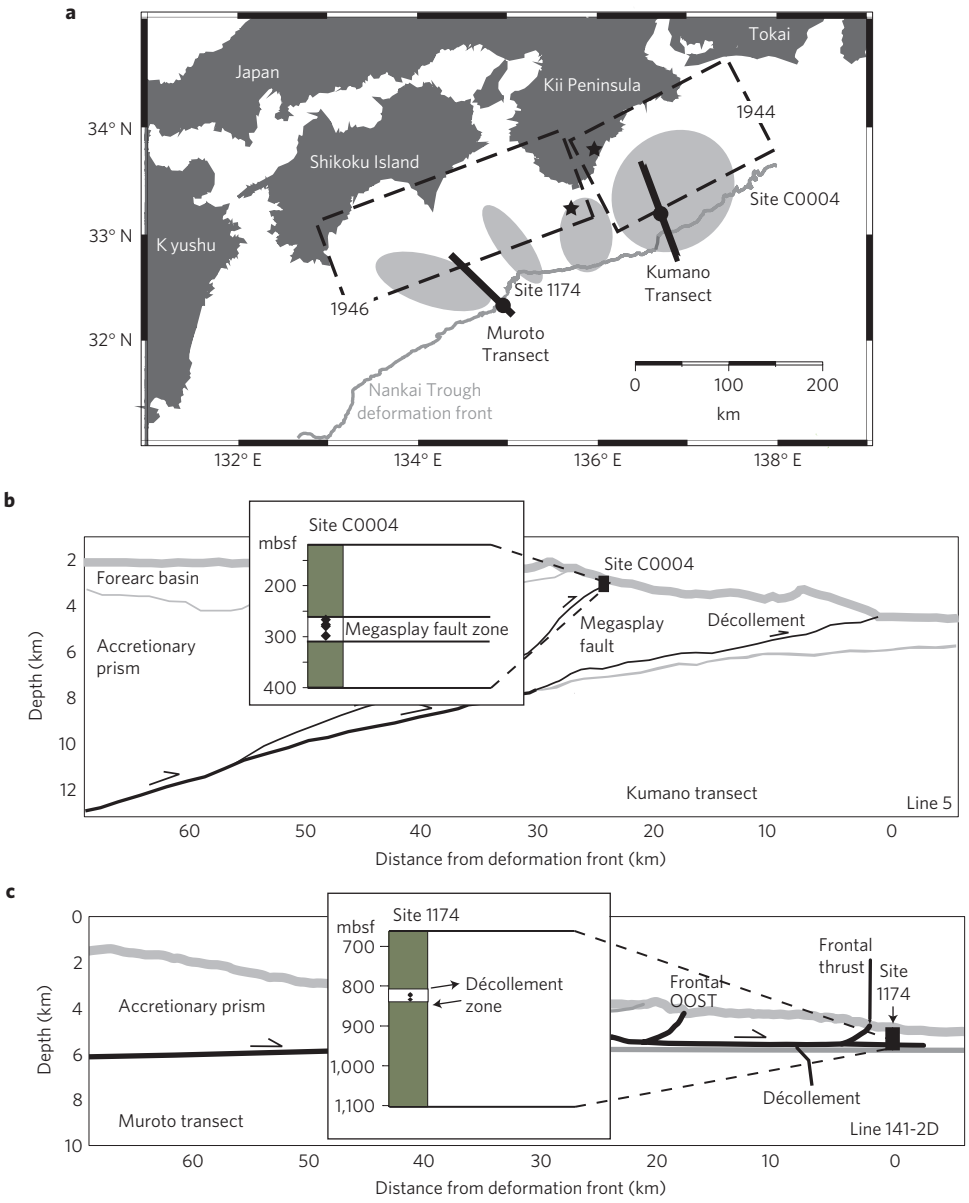

Figure 1 | Geologic setting of the Nankai subduction zone. a, Map of the Nankai area, offshore Japan, showing the locations of drilling sites C0004 (megasplay) and 1174 (décollement). Grey ovals indicate clusters of VLF earthquakes identified in ref. 8. Also shown are rupture areas (dashed boxes) and epicentres (stars) of the 1944 Tonankai and 1946 Nankaido earthquakes. **b**, Cross-section of the Kumano transect, showing the location of samples tested from the megasplay fault zone. **c**, Cross-section of the Muroto transect, showing the location of samples tested from the décollement zone. Figure modified from ref. 24.

perturbation, D_c, is usually $\sim\leq$100 μm (ref. 17). Slip-dependent friction trends over sliding distances of ~1 mm are observed experimentally, but typically assumed to reflect background trends that do not affect sliding stability[25]. We investigate the effects of these long-term trends by measuring the slip dependence of friction, defined by the parameter $\eta = \mathrm{d}\mu/\mathrm{d}x$ (mm^{-1}) measured from a linear fit to the last ~300 μm of each 800 μm velocity step (Fig. 2c). In our experiments, this slip weakening occurs beyond the initial effects of slip velocity perturbations; therefore, although η is determined from velocity steps it is distinct from standard RSF behaviour.

We find that negative values of η are common for samples from Nankai, indicating slip-weakening behaviour (Fig. 3b). Minimum values of η coincide with the minima in $a-b$ in the velocity range ~0.3–3 μm s^{-1}. Negative η could result in net weakening and slip instability, if initial velocity-strengthening behaviour is overcome by longer term slip weakening beyond a critical sliding distance W:

$$W = \frac{(a-b)\ln(V/V_o)}{-\eta}$$

(Fig. 2). As W is calculated from $a-b$ and η, it also exhibits minimum values in the range 0.3–3 μm s^{-1} (Fig. 3c). If $a-b$ and/or W are small, unloading of the fault zone during slip is dominated by the long-term slip-weakening rate η rather than by RSF parameters. In this case, a stiffness criterion analogous to equation (1) may be expressed as:

$$K < K_c^* = -\eta\sigma_n'$$

where K_c^* is the critical stiffness for slip instability by slip weakening.

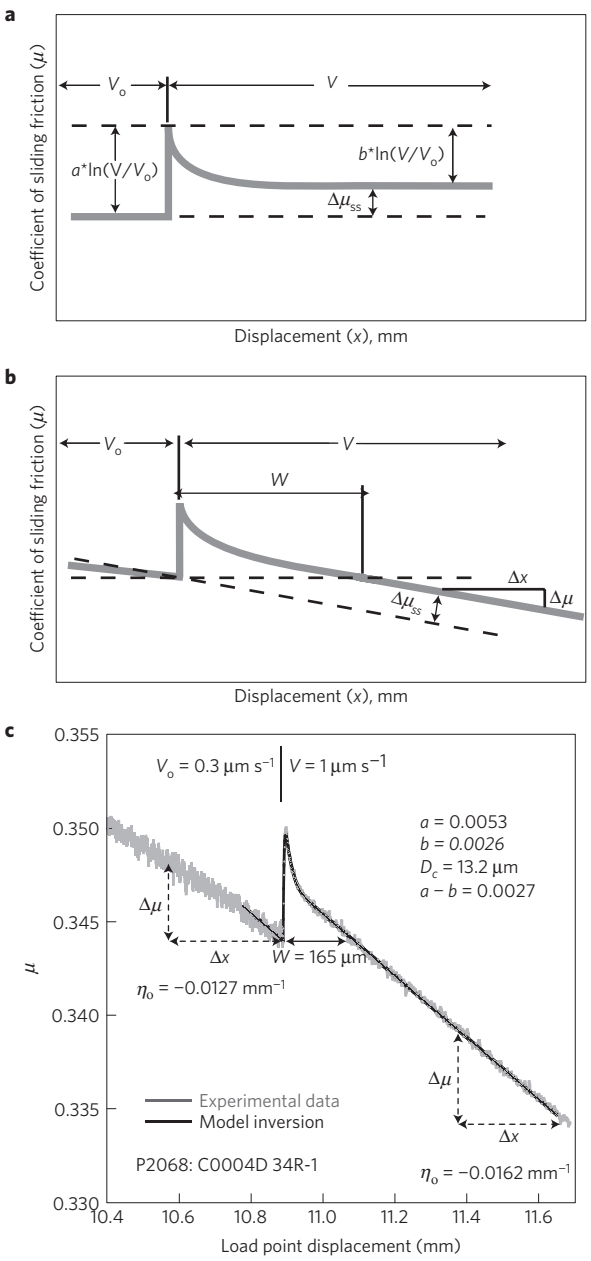

Figure 2 | Determination of important friction parameters. a, Illustration of the changes in steady-state coefficient of friction ($\Delta\mu_{ss}$) in response to an increase in load point velocity from V_o to V. **b**, The same as in **a** with a slip-weakening trend superimposed. W is the critical slip weakening distance. **c**, An example of experimental data (grey) overlain by an inverse model (black) used to extract the constitutive friction parameters a, b, $a-b$ and D_c (ref. 21). Slip weakening rates before (η_o) and after the velocity step (η) are determined by the change in friction ($\Delta\mu$) per change in displacement (Δx). This sample is from within the Nankai megasplay fault zone.

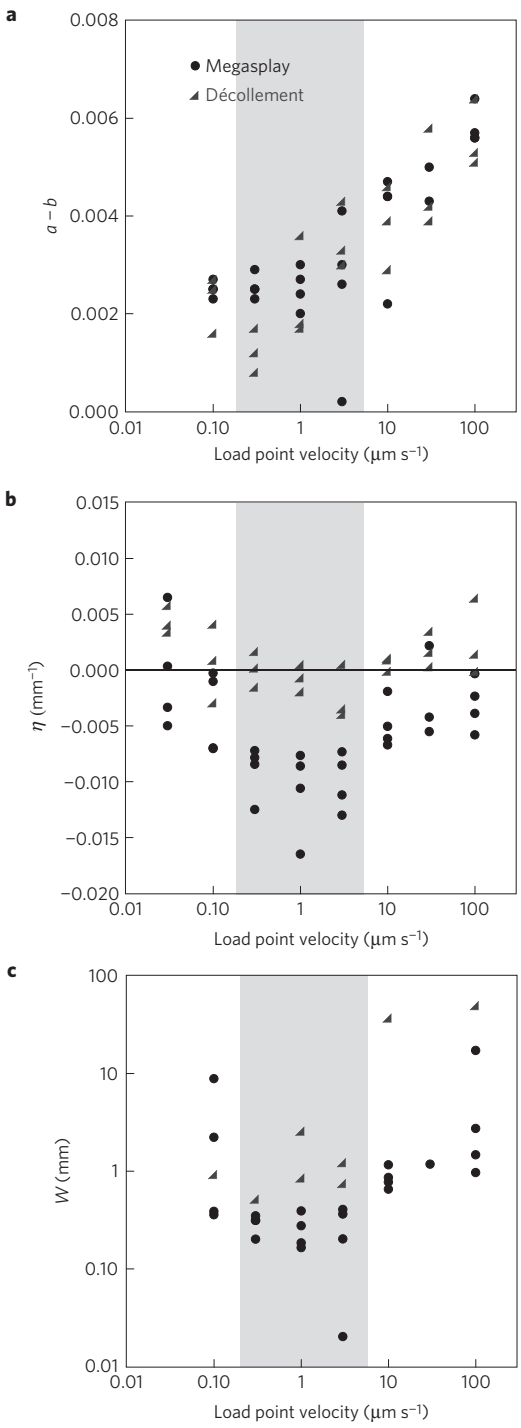

Figure 3 | Summary of experimental results. a–**c**, RSF parameter $a-b$ (**a**), slip-weakening rate η (**b**) and critical slip-weakening distance W (**c**) as a function of upstep sliding velocity from friction experiments for samples from the megasplay fault zone (black circles) and décollement (grey triangles). Values of $a-b$ and W are reported in terms of the upstep velocity V (rather than V_o).

For natural faults, the stiffness criterion defines the minimum size a slipping patch must attain before instability can nucleate. This patch is usually treated as an elliptical crack with a minimum half length, L_c (ref. 18):

$$L_c = \frac{E}{2(1-\nu^2)K_c}$$

where E is the Young's modulus of the wall rock, and ν is the Poisson's ratio. Substituting K_c^* for K_c and using values of $\eta = -0.0165\,\mathrm{mm}^{-1}$ for the Nankai megasplay and $-0.0040\,\mathrm{mm}^{-1}$ for the décollement (the lowest values we observe; Fig. 3), we estimate the minimum patch size required for instability (L_c). We use a value of $\sigma_n' = 10$–20 MPa, which is both near our experimental condition (25 MPa), and corresponds to the estimated *in situ* effective stress in the source region of well-located VLF events with distinguishable P-wave arrivals[15]. On the basis of sonic velocity

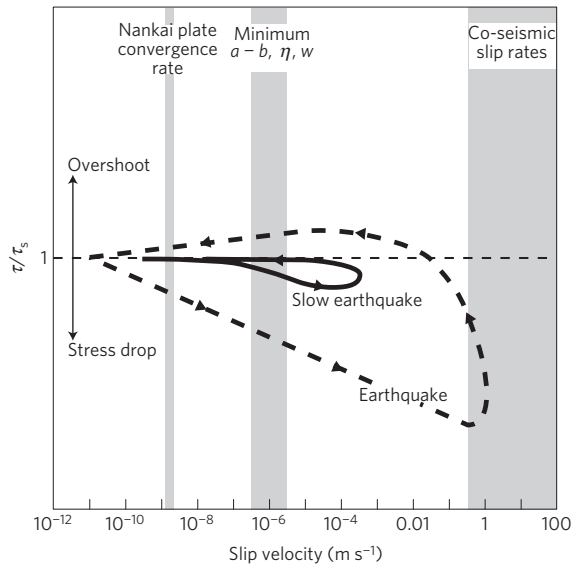

Figure 4 | Schematic illustration of fault behaviour. Comparison of the stress paths followed during a normal earthquake (thick dashed line) and slow earthquake (solid line) as a function of slip velocity. τ is the initial shear strength of the fault before the event, and τ_s is the shear strength during slip.

measurements in a sample located 22 m below the megasplay fault zone that yield a bulk modulus of 6.70 GPa and shear modulus of 1.30 GPa (ref. 14), E and ν of the fault surroundings are 3.66 GPa and 0.41, respectively. The resulting L_c are 6.7–13.3 m for the megasplay and 27.5–55.0 m for the décollement.

Shallow VLF events in Nankai have seismic moments $M_o = \sim 4 \times 10^{14} - 2 \times 10^{15}$ Nm (ref. 5), corresponding to $L_c = 37$–63 m based on standard scaling relations[26]. Thus, the nucleation patch size of these VLF earthquakes is compatible with constraints provided by our experimental data using the natural material likely to host such events. In comparison to the megasplay samples, décollement material exhibits less slip weakening, and slip strengthening in some cases (Fig. 3b). Thus, the décollement zone requires a larger nucleation patch for instability relative to the megasplay, or may not allow generation of slow earthquakes by this mechanism. This suggests that the megasplay is more likely to host these events[8].

Our data also highlight that maximum values of slip weakening in the velocity range ~0.3–3 μm s^{-1} would facilitate acceleration to higher slip rates. However, the combination of increasing $a-b$ and decreasing η at higher slip velocities favours stable sliding and therefore we anticipate that any initiating slip event would be arrested before reaching typical seismic slip velocities (~1 m s^{-1}; Fig. 4). This is consistent with estimated maximum slip velocities of ~0.05–2 mm s^{-1} for shallow Nankai VLF events[9]. This effect is also consistent with the low stress drops of such events compared to normal earthquakes, and with the lack of dynamic overshoot (Fig. 4). It may also explain why they radiate less high-frequency energy than normal earthquakes[1,8,9]. Stress drops generally cluster around 10 kPa for many types of slow slip event[27]; for VLF earthquakes in Nankai they are estimated to be ~0.1–10 kPa, 0.1–1% of that expected for normal earthquakes[9].

Our data imply that during the initiation of slow earthquakes, a large fraction of the total displacement may accumulate at low velocities (<0.3 μm s^{-1}) because larger slip is required to achieve net weakening if the slip-weakening rate is small. This would produce longer rise times because the seismic moment, and therefore the stress drop, is proportional to the square of the rise time for slow slip events[22]. Very long rise times have been reported for slow slip events on the San Andreas fault[21] and the Bungo Channel region of Japan[23]. Analyses of normal earthquakes[28] and aftershock sequences[29] have suggested that rupture initiation is characterized by a slow nucleation phase, with an extended rise time and low rate of moment release. Therefore, dynamic and quasi-dynamic slow slip events may start as normal earthquakes but are slowed or terminated during the nucleation phase. Our experimental observations offer one possible explanation for the arrest of slow earthquakes that might act separately or in concert with other suggested mechanisms[5,12,19].

Several numerical modelling studies have simulated slow slip events using existing RSF laws[5–7,20], preferentially targeting events at the downdip limit of the seismogenic zone. They typically incorporate two processes to limit slip speed: a switch from velocity-weakening to velocity-strengthening behaviour during dynamic slip nucleation; and extremely low σ_n' speculated to result from near-lithostatic pore-fluid pressure. The velocity-dependent behaviour is based on observed frictional properties of analogue materials such as granite[6,25], halite[7] or gabbro[6]. Another mechanism is dilatancy hardening, where velocity-weakening material is strengthened during slip by transiently reduced pore pressure[5]. Elevated pore pressure is often cited as a requirement for emergent slow slip in numerical models because low σ_n' favours stable or conditionally stable slip rather than dynamic instabilities resulting in earthquakes[18] (equation (1)). This is consistent with seismic tomography studies revealing high V_p/V_s ratios and high Poisson's ratio at the base of the seismogenic zone[3] and with elevated pore pressure estimated from low P-wave velocity in the source region of VLF events[15].

At Nankai, major fault zones at shallow depths are composed of 37–65% clay minerals[13,14] and are consistently velocity strengthening at sub-seismic slip rates, suggesting that unstable slip should not be expected[3,24]. The slip-weakening behaviour we report may be a viable mechanism for the generation of slow slip events or VLF earthquakes, without requiring velocity-weakening behaviour. Elevated pore pressure and concomitant low effective stress have been documented along the shallow décollement and in the accretionary wedge[15,30], which may modulate these slip events, but we show that it is not a necessary condition for their generation. The mechanism responsible for velocity-dependent friction over shorter distances characteristic of RSF parameters is thought to be related to grain-scale processes[16,25]. We posit that slip weakening in our samples is related to shear fabric development and microstructural features such as Riedel or boundary shears within the fault zone[31].

Received 30 August 2012; accepted 9 April 2013; published online 12 May 2013

References

1. Ide, S., Beroza, G. C., Shelly, D. R. & Uchide, T. A scaling law for slow earthquakes. *Nature* **447,** 76–79 (2007).
2. Peng, Z. & Gomberg, J. An integrated perspective of the continuum between earthquakes and slow-slip phenomena. *Nature Geosci.* **3,** 599–607 (2010).
3. Hyndman, R. D. in *The Seismogenic Zone of Subduction Thrust Faults* (eds Dixon, T. H. & Moore, J. C.) 15–40 (Columbia Univ. Press, 2007).
4. Chapman, J. S. & Melbourne, T. I. Future Cascadia megathrust rupture delineated by episodic tremor and slip. *Geophys. Res. Lett.* **36,** L22301 (2009).
5. Segall, P., Rubin, A. M., Bradley, A. M. & Rice, J. R. Dilatant strengthening as a mechanism for slow slip events. *J. Geophys. Res.* **115,** B12305 (2010).
6. Liu, Y. & Rice, J. R. Slow slip predictions based on granite and gabbro friction data compared to GPS measurements in northern Cascadia. *J. Geophys. Res.* **114,** B09407 (2009).
7. Shibazaki, B. & Shimamoto, T. Modeling of short-interval silent slip events in deeper subduction zone interfaces considering the frictional properties at the unstable–stable transition regime. *Geophys. J. Int.* **171,** 191–205 (2007).
8. Obara, K. & Ito, Y. Very low frequency earthquakes excited by the 2004 off the Kii Peninsula earthquakes: A dynamic deformation process in the large accretionary prism. *Earth Planets Space.* **57,** 321–326 (2005).
9. Ito, Y. & Obara, K. Very low frequency earthquakes within accretionary prisms are very low stress-drop earthquakes. *Geophys. Res. Lett.* **33,** L09302 (2006).
10. Sugioka, H. *et al.* Tsunamigenic potential of the shallow subduction plate boundary inferred from slow seismic slip. *Nature Geosci.* **5,** 414–418 (2012).

11. Kodaira, S. *et al.* High pore fluid pressure may cause silent slip in the Nankai Trough. *Science* **304,** 1295–1298 (2004).
12. Rubin, A. M. Designer friction laws for bimodal slow slip propagation speeds. *Geochem. Geophys. Geosyst.* **12,** Q04007 (2011).
13. Moore, G. F. *et al. Proc. ODP, Init. Repts.* Vol. 190, College Station, TX (Ocean Drilling Program, 2001).
14. Kinoshita, M. *et al. Proc. IODP* Vols 314/315/316, Washington, D.C. (Integrated Ocean Drilling Program Management International, 2009).
15. Kitajima, H. & Saffer, D. M. Elevated pore pressure and anomalously low stress in regions of low frequency earthquakes along the Nankai subduction megathrust. *Geophys. Res. Lett.* **39,** L23301 (2012).
16. Dieterich, J. H. in *Mechanical Behavior of Crustal Rocks* Vol. 24 (eds Carter, N. L. *et al.*) 102–120 (Geophys. Monogr. Ser., 1981).
17. Marone, C. Laboratory-derived friction laws and their application to seismic faulting. *Annu. Rev. Earth Planet. Sci.* **26,** 643–696 (1998).
18. Scholz, C. H. *The Mechanics of Earthquakes and Faulting* 2nd edn (Cambridge Press, 2002).
19. Roy, M. & Marone, C. Earthquake nucleation on model faults with rate- and state-dependent friction: Effects of inertia. *J. Geophys. Res.* **101,** 13919–13932 (1996).
20. Perfettini, H. & Ampuero, J-P. Dynamics of a velocity-strengthening fault region: Implications for slow earthquakes and postseismic slip. *J. Geophys. Res.* **113,** B09411 (2008).
21. Linde, A. T., Gladwin, M. T., Johnston, M. J. S., Gwyther, R. L. & Bilham, R. G. A slow earthquake sequence on the San Andreas fault. *Nature* **383,** 65–68 (1996).
22. Crescentini, L., Amoruso, A. & Scarpa, R. Constraints on slow earthquake dynamics from a swarm in Central Italy. *Science* **286,** 2132–2134 (1999).
23. Hirose, H., Hirahara, K., Kimata, F., Fujii, N. & Miyazaki, S. A slow thrust slip event following the two 1996 Hyuganada earthquakes beneath the Bungo Channel, southwest Japan. *Geophys. Res. Lett.* **26,** 3237–3240 (1999).
24. Ikari, M. J. & Saffer, D. M. Comparison of frictional strength and velocity dependence between fault zones in the Nankai accretionary complex. *Geochem. Geophys. Geosyst.* **12,** Q0AD11 (2011).
25. Blanpied, M. L., Marone, C. J., Lockner, D. A., Byerlee, J. D. & King, D.P. Quantitative measure of the variation in fault rheology due to fluid-rock interactions. *J. Geophys. Res.* **103,** 9691–9712 (1998).
26. Ohnaka, M. A physical scaling relation between the size of an earthquake and its nucleation zone size. *Pure Appl. Geophys.* **157,** 2259–2282 (2000).
27. Brodsky, E. E. & Mori, J. Creep events slip less than ordinary earthquakes. *Geophys. Res. Lett.* **34,** L16309 (2007).
28. Ellsworth, W. L. & Beroza, G. C. Seismic evidence for an earthquake nucleation phase. *Science* **286,** 851–855 (1995).
29. Iio, Y. Observations of the slow initial phase generated by microearthquakes: Implications for earthquake nucleation and propagation. *J. Geophys. Res.* **100,** 15333–15349 (1995).
30. Saffer, D. M. & Tobin, H. J. Hydrogeology and mechanics of subduction zone forearcs: Fluid flow and pore pressure. *Annu. Rev. Earth. Planet. Sci.* **39,** 157–186 (2011).
31. Logan, J. M., Dengo, C. A., Higgs, N. G. & Wang, Z. Z. in *Fault Mechanics and Transport Properties of Rocks* (eds Evans, B. & Wong, T-F.) 33–67 (Academic, 1992).

Acknowledgements

We thank N. De Paola for constructive comments, which improved this manuscript. This work was supported by NSF awards OCE-0451602, OCE-0752114 and OCE-0648331 to D.M.S. and C.M., and by Deutsche Forschungsgemeinschaft (DFG) through the MARUM Research Center.

Author contributions

M.J.I conducted experiments and data analysis. All authors contributed to planning and writing the manuscript, and providing support.

Additional information

Reprints and permissions information is available online at www.nature.com/reprints. Correspondence and requests for materials should be addressed to M.J.I.

Competing financial interests

The authors declare no competing financial interests.